ELSEVIER

www.elsevier.nl/locate/jelechem

Journal of Electroanalytical Chemistry 483 (2000) 7–17

Journal of Electroanalytical Chemistry

Review

Studies of charge transfer at liquid | liquid interfaces and bilayer lipid membranes by scanning electrochemical microscopy☆

Shigeru Amemiya, Zhifeng Ding, Junfeng Zhou, Allen J. Bard *

Department of Chemistry and Biochemistry, The University of Texas at Austin, Austin, TX 78712, USA

Received 18 November 1999; received in revised form 3 January 2000; accepted 11 January 2000

Abstract

The principles of scanning electrochemical microscopy (SECM) and its application to studies of electron transfer at the interface between two immiscible electrolyte solutions are reviewed. The results of SECM measurements with a number of redox couples at the bare liquid | liquid interface or an interface with a lipid monolayer suggest that the electron transfer follows that predicted by Marcus theory, with evidence for an inverted region. The SECM can also be used to probe processes at bilayer lipid membranes.

Keywords: Scanning electrochemical microscopy; Bilayer lipid membranes; Electron transfer; Immiscible electrolyte solutions

1. Introduction

We review here the application of the scanning electrochemical microscope (SECM) to studies of the interface between two immiscible electrolye solutions (ITIES) and the bilayer lipid membrane (BLM). Previous studies of charge (electron and ion) transfer at the ITIES have been reviewed [1], and this topic is discussed in several of the papers in this issue. In most cases these studies have involved four-electrode systems, where the current is measured when a potential is applied across the interface. With the SECM, all electrodes are contained in a single phase, and the potential across the ITIES is controlled by the composition of the two liquid phases. The rate of electron transfer is determined by measuring the feedback current at an ultramicroelectrode, as described below.

2. Principles of SECM

The theory, methodology, and instrumentation in SECM have been reviewed [2,3]. The basic concept of interest in connection with measurements at the ITIES is that of the tip feedback current. When the ultramicroelectrode tip is far from any surface, the tip current, $i_{T,\infty}$, for the reaction $Ox + ne^- \rightarrow Red$, is given by:

$$i_{T,\infty} = 4nFDCa \quad (1)$$

where n is the number of electrons involved in the electrode reaction, F is the Faraday constant, D is the diffusion coefficient and C the concentration of the electroactive reactant, Ox, and a is the radius of the ultramicroelectrode tip (assumed to be a disk). When the tip is close to a surface, the tip current, i_T, is perturbed by blockage of diffusion of Ox to the tip by the substrate and by reactions that occur at the substrate surface. If the substrate surface is an insulator or a surface where the tip generated product, Red, does not react, $i_T < i_{T,\infty}$. This is termed negative feedback. The curve of i_T versus tip–substrate separation, d, is called an approach curve (Fig. 1), and these can be obtained by digital simulation. If the oxidation of Red to Ox occurs at the substrate, the current will be larger

☆ Paper presented at the Euroconference on Modern Trends in Electrochemistry of Molecular Interfaces, Finland, 28 August–3 September 1999.

* Corresponding author. Tel.: +1-512-4713761; fax: +1-512-4710088.

E-mail address: ajbard@mail.utexas.edu (A.J. Bard)

0022-0728/00/$ - see front matter
PII: S0022-0728(00)00021-8

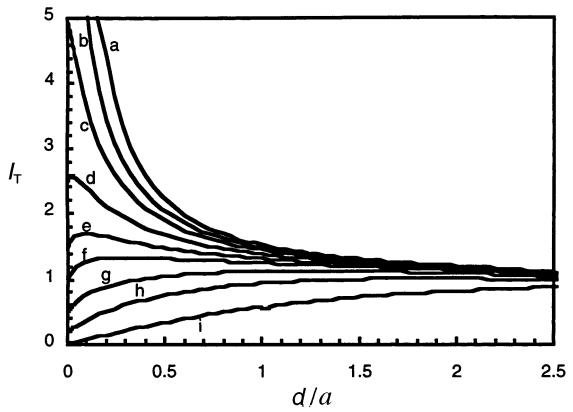

Fig. 1. Approach curves ($i_T/i_{T,\infty}$ vs. d/a) for a totally irreversible reaction at the interface, k. $I_T = i_T/i_{T,\infty}$. From top to bottom, k (cm s^{-1}) is: (a) 1; (b) 0.5; (c) 0.1; (d) 0.025; (e) 0.015; (f) 0.01; (g) 0.005; (h) 0.002; (i) 0.0001. Curve (a) is identical to that for mass transfer control and curve (i) for an insulating substrate.

than that seen in the negative feedback approach curve, depending on the rate of the reaction. For sufficiently high rate constants, k, for this oxidation reaction on the substrate, i_T must be greater than $i_{T,\infty}$ (positive feedback). Typical calculated approach curves as a function of k are shown in Fig. 1. By comparing an experimental approach curve to theoretical ones, the rate constant for a reaction at the substrate can be obtained.

3. SECM measurement of ET rate constants at the ITIES

In contrast to the conventional studies of the ITIES at externally biased polarizable interfaces, the SECM experiments of electron transfer (ET) at the interface are carried out at an interface where a common ion in both phases produces a constant potential drop across the interface [4]. Because all electrodes are in a single phase, it is possible to avoid the problems of the large interfacial capacitance and uncompensated *IR* drop within the phases and across the interface. Furthermore, use of an ITIES with fixed and adjustable interfacial potentials enables SECM measurements to be carried out over a wide range of driving forces without the limitation of the potential window. This can be contrasted with cyclic voltammetry with a four-electrode system, where the ET reaction must be in a potential window that normally has a range of only about $\pm$ 0.4 V [1]. These advantages of SECM allow for a quantitative understanding of ET kinetics at the ITIES, as discussed below.

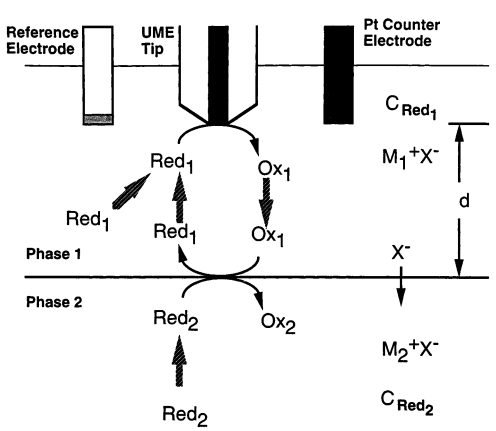

Fig. 2. Schematic diagram of SECM measurements of ET at the ITIES. Species Red_1 and Ox_1 are confined to phase 1, while species Red_2 and Ox_2 are present in phase 2. The electrolytes $M_1^+X^-$ and $M_2^+X^-$ determine the potential drop across the interface. Mass transfer is indicated by the thick arrows.

3.1. Four stages of the overall SECM process for an ET reaction at the ITIES

The SECM measurements of ET at the ITIES are shown schematically in Fig. 2. When the ultramicroelectrode (UME) tip is positioned close to the interface, ET between the redox-active species in phase 2 (Red_2) and the tip-generated species in phase 1 (Ox_1) occurs at the interface and regenerates the original species in phase 1 (Red_1):

$$Ox_1 + Red_2 \rightarrow Ox_2 + Red_1 \quad (2)$$

The regenerated species produces positive feedback at the tip, enhancing the steady-state current. Because in SECM measurements the interface is poised by the potential determining ions that can partition between the two phases, electroneutrality in both phases is maintained by ion transfer (IT) following the ET (e.g. transfer of X^- from phase 1 to phase 2 in Fig. 2).

Quantitative fitting of the SECM approach curves produces the rate constants of the charge transfer processes at the interface [2,3]. In SECM studies of ET reactions at the ITIES, four types of processes (whose rates are represented as currents) can affect the tip current [5]:

1. mediator diffusion limiting current in phase 1, i_T^c,
2. limiting current of heterogeneous electron transfer reaction, i_{ET},
3. diffusion limiting current of the redox species in phase 2, i_d,
4. charge compensation current by IT at the interface, i_{IT}.

The kinetics of such an ET reaction (Eq. (2)) can be evaluated microscopically from the measured tip current. The electrical current across the ITIES (i_S) caused by this multistage serial process can be expressed as [6]:

$$1/i_S = 1/i_T^c + 1/i_{ET} + 1/i_d + 1/i_{IT} \quad (3)$$

Any of the four stages can be rate-limiting, but our main concern is to investigate the heterogeneous ET reaction. The diffusion processes in both phases can be

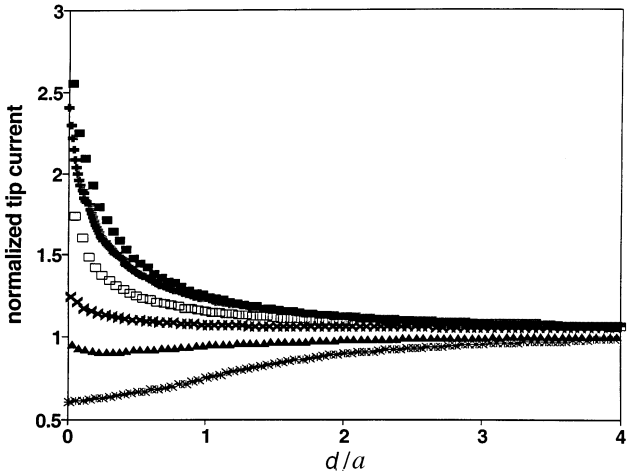

Fig. 3. Effect of the concentration of FcCOONa in the aqueous phase on the shape of current–distance curves. $c_{FcCOONa}$ was, from top to bottom, 0.25, 0.5, 0.8, 1.0, 2.0, and 5.0 mM. Aqueous solution also contained 0.1 M KCl; NB contained 75 mM Fc. Reprinted from Ref. [5]. Copyright 1995 American Chemical Society.

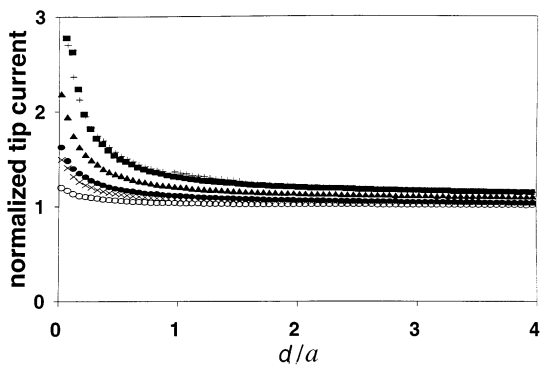

Fig. 4. Effect of the concentration of TEAP on the shape of current–distance curves. The concentration of TEAP in both NB and water was (○) 0; (×) 0.01; (●) 0.1; (▲) 1; (■) 10, and (+) 75 mM. Aqueous solution also contained 1 M KCl; NB contained 75 mM Fc. Reprinted from Ref. [5]. Copyright 1995 American Chemical Society.

evaluated quantitatively by SECM theories [3,7]. However, no theoretical treatment has been proposed for the separation between IT and ET kinetics, although IT-coupled ET reactions at the ITIES have been studied theoretically and experimentally [8–10]. Thus, possible IT limitations on the whole process were investigated to extract ET kinetics from the SECM approach curves.

3.2. Separation of IT and ET by SECM

The SECM current allows discrimination between ET and IT and allows the determination of ET rate constants [5]. The possibility of separating the ET and IT processes was studied for a slow ET reaction between FcCOONa in water (phase 1) and Fc in nitrobenzene (NB) (phase 2):

$$FcCOO^-\ (w) - e^- \rightarrow FcCOO\ (w)\ (tip) \quad (4)$$

$$Fc\ (o) + FcCOO\ (w) \rightarrow Fc^+\ (o) + FcCOO^-\ (w)\ (ITIES) \quad (5)$$

As shown in Fig. 3, one can see that in the absence of a supporting electrolyte in NB, the normalized tip current decreases markedly with an increase in the concentration of FcCOONa in water. This cannot be attributed to ET limitations because the rate of the ET increases proportionally to the concentration of the reactant (see Eq. (6)). Since the redox process in NB is an oxidation, the tip-injected positive charges must be compensated by IT such as cation expulsion from, or anion injection into, the NB. With no excess of supporting electrolyte in the NB, the overall process will be under mixed ET and IT kinetic control. Indeed, the approach curves in Fig. 3 were fit well by an empirical equation, where the limiting IT current was assumed to be a sum of two terms: the transfer of Fc^+ from the NB and of aqueous anions (Cl^- and $FcCOO^-$) into the NB.

Fig. 4 provides further evidence that IT limitations come from the pronounced dependence of the shape of the approach ($i_T - d$) curves with concentration of tetraethylammonium perchlorate (TEAP) as a supporting electrolyte at the same ratio of the TEAP concentration in the two phases at the beginning of the experiments. The initial increase in IT current was most likely caused not by a direct contribution of the added TEAP to IT, but rather by a change in the potential drop across the ITIES and this, therefore, produced an increase in the potential-dependent IT rate constant. Subsequent changes in TEAP concentration in both phases should not have affected the Galvani potential difference at the interface, $\Delta_w^o\phi$, because the ratio of the concentrations in the two phases does not change (Eq. (9)) [4]. However, the normalized feedback current increased markedly with an increase of TEAP concentration up to about 10 mM. At higher values, the shape of the curves became independent of the concentration, so that the two upper curves in Fig. 4 obtained with 10 and 75 mM of TEAP, respectively, are practically indistinguishable. This result indicates that at sufficiently high electrolyte concentrations, the overall process is limited by slow ET.

3.3. ET rate constants

The bimolecular ET rate constant, k_{12}, can be determined by the same approach as that applied for an SECM study of heterogeneous ET on an electrode [3]. When the bulk concentration of the reactant in phase 2, c_{Red2}, is in excess of the reactant in phase 1, c_{Red1}, (i.e. $c_{Red2} \gg c_{Red1}$, to exclude the possibility of diffusion limitation in the second phase), the theory developed pre-

viously to extract the kinetic parameter is applicable to the analysis of the $i_T - d$ curves [5]. The apparent heterogeneous rate constant, k_f, that is determined by SECM approach curves is:

$$k_f = k_{12} c^i_{Red2} \quad (6)$$

where c^i_{Red2} is the interfacial concentration of Red_2. Because $c^i_{Red2} = c_{Red2}$, a bimolecular rate constant, k_{12}, of 0.6 cm M^{-1} s^{-1} was obtained by fitting the approach curves in Fig. 4 for the cases of ET limitation [5].

The measured value can be interpreted either by assuming a sharp, planar boundary between the two solvents or by adopting a reaction-layer-type formalism [11–14]. The calculated values can be used to express quantitatively the rate of the interfacial ET in a form that can be compared with experimental results [11–15] and can be used to assess the thickness of the interface. Preliminary results from SECM suggest that the thickness of a liquid | liquid interface for the solvents studied is of the order of a few nanometers [5].

4. Driving force dependence of the ET rate at the ITIES

Of particular interest in studies of the kinetics of ET reactions is the driving-force dependence of the rate constant. The dependence of k_{12} on the energy of activation, $\Delta G^{\neq}$, is:

$$k_{12} = \text{const} \ \exp(-\Delta G^{\neq}/RT) \quad (7)$$

When the overpotential is low, a Butler–Volmer type approximation will be followed:

$$-\Delta G^{\neq} = \alpha F(\Delta E^{\circ} + \Delta^{o}_{w}\phi) \quad (8)$$

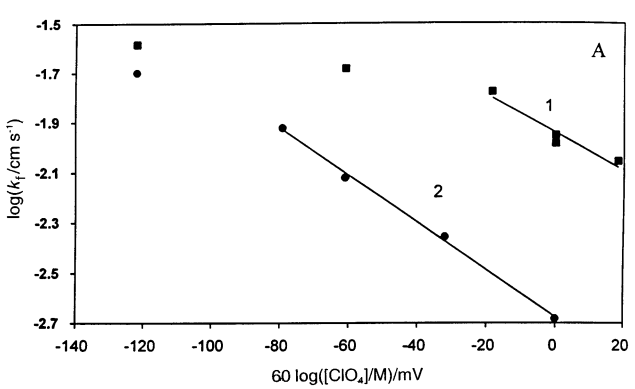

Fig. 5. Dependence of the effective heterogeneous rate constant on potential drop across the ITIES at (1) 50 and (2) 5 mM concentrations of $Ru(CN)_6^{4-}$ in an aqueous solution containing 0.1 M NaCl and different concentrations of $NaClO_4$. Benzene was 0.5 mM in ZnPor and 0.25 M in $THAClO_4$. Reprinted from Ref. [16]. Copyright 1996 American Chemical Society.

where ΔE° is the difference between the standard potentials of two redox couples, and α is the transfer coefficient. The dependence of the ET rate constant on the two types of driving forces, i.e. $\Delta^{o}_{w}\phi$ and ΔE°, were investigated as follows [16,17].

In SECM experiments at the ITIES, the Galvani potential difference is determined by partitioning of a common ion [7,16–18] or a salt [5] between the two phases. A Nernst-form equation for a partitioning ion i in the two phases can be written as:

$$\Delta^{o}_{w}\phi = \Delta^{o}_{w}\phi^{o'}_{i} + \frac{RT}{z_i F}\ln\left(\frac{c^{w}_{i}}{c^{o}_{i}}\right) \quad (9)$$

where $\Delta^{o}_{w}\phi^{o'}_{i}$ and z_i are the formal transfer potential and the charge of the partitioning ion, respectively, and c^{w}_{i} and c^{o}_{i} are the concentrations of the partitioning ion in the two phases. Thus, if both supporting electrolytes in the two phases contain ClO_4^-, for example, as the only common ion, the interfacial potential drop can be controlled quantitatively and varied by changing the ratio of concentrations of ClO_4^- in water and the organic phase. This approach was used to study the potential dependence of the rate constant for ET at the ITIES, without biasing the interface externally. The SECM measurement was carried out for the case of ZnPor in benzene (phase 1) and $Ru(CN)_6^{4-}$ in water as Red_2 on the basis of the following reactions:

$$ZnPor\ (o) - 1e^- \rightarrow ZnPor^+\ (o)\ (tip) \quad (10)$$

$$ZnPor^+\ (o) + Red_2\ (w)$$

$$\rightarrow ZnPor\ (o) + Ox_2\ (w)\ (ITIES) \quad (11)$$

$c^{o}_{ClO_4^-}$ was maintained constant in these experiments, and $\Delta^{o}_{w}\phi$ shifted by 59 mV to more negative values with each decade increase in $c^{w}_{ClO_4^-}$. Plots of $\log k_f$ versus $\log c^{w}_{ClO_4^-}$, i.e. Tafel-type plots, at different concentrations of $Ru(CN)_6^{4-}$ are shown in Fig. 5. At higher $c^{w}_{ClO_4^-}$, corresponding to less positive $\Delta^{o}_{w}\phi$, the plots were linear and the transfer coefficient was similar for different concentrations of $Ru(CN)_6^{4-}$ ($\alpha = 0.49 \pm 0.1$ and 0.56 ± 0.05 for 50 and 5 mM $Ru(CN)_6^{4-}$, respectively [16]). On the other hand, at lower $c^{w}_{ClO_4^-}$, corresponding to a more positive $\Delta^{o}_{w}\phi$, the ET rate was limited by the rate of diffusion of the ZnPor couple and the curves tended to level off. The linear Tafel plots with transfer coefficients α close to 0.5 suggest that conventional ET theory (a Butler–Volmer model) is applicable to the liquid | liquid interface when the driving force is not too high. However, recent SECM studies by Liu and Mirkin [19] showed that the ET rate at the ITIES is independent of $\Delta^{o}_{w}\phi$ when the redox reactant in the organic phase is an electrically neutral species. Thus, we cannot exclude the possibility that the linear dependence of $\log k_f$ versus $\Delta^{o}_{w}\phi$ for ET involving a charged organic redox species ($ZnPor^+$ in Eq. (11)) is due to the diffuse layer effect similar to a Frumkin effect at metal electrodes [20].

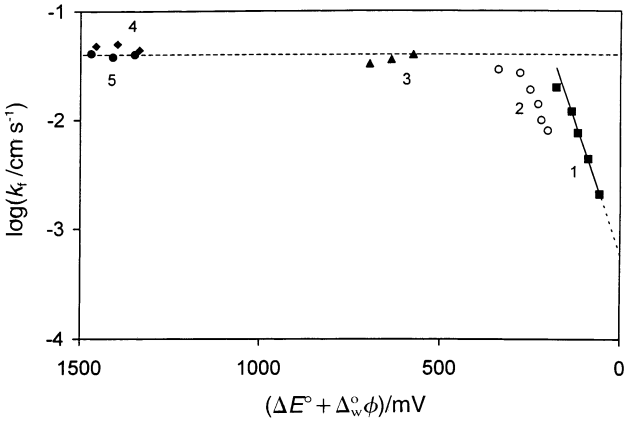

Fig. 6. Potential dependence of the rate of ET between $ZnPor^+$ in benzene and various aqueous redox species. The abscissa plots the driving force for ET given in Eq. (3). The aqueous solution contained 0.01–2 M $NaClO_4$ and 7 mM of: (1) $Ru(CN)_6^{4-}$; (2) $Mo(CN)_8^{4-}$; (3) $Fe(CN)_6^{4-}$, (4) Co(II) sepalchrate, and (5) V^{2+}. The aqueous supporting electrolyte was (1–4) 0.1 M NaCl and (5) 0.5 M H_2SO_4. A benzene solution contained 0.5 mM ZnPor and 0.25 M $THAClO_4$. Horizontal dashed line shows the diffusion limit for the ET rate measurements by SECM with a 25-μm tip (~ 0.03 cm s^{-1}). The rate constants are calculated using the diffusion coefficient of ZnPor, $D = 4 \times 10^{-6}$ cm^2 s^{-1}. Reprinted from Ref. [17]. Copyright 1997 American Chemical Society.

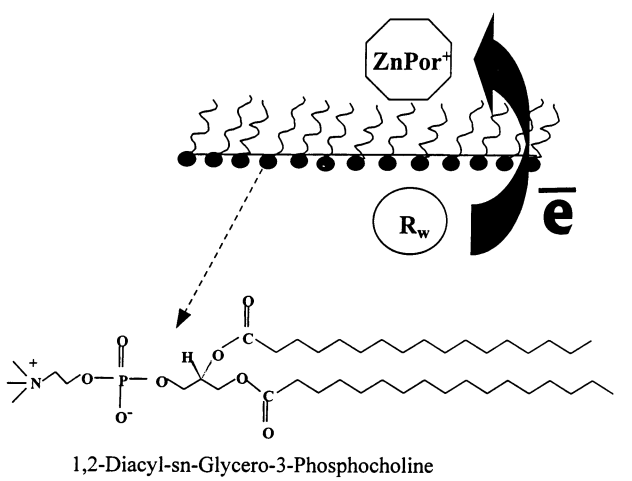

Fig. 7. The ITIES modified by a monolayer of phospholipid. The inset shows the structure of synthetic phosphatidyl choline lipids. Reprinted from Ref. [17]. Copyright 1997 American Chemical Society.

The potential dependence of the ET rate constant, as shown above, is consistent with the linear driving force dependence of the activation energy expected at low overpotential (Eq. (8)). However, the driving force for the interfacial ET reaction should include not only the $\Delta^\circ_w\phi$ term but also the difference of standard potentials of the organic and aqueous redox mediators as shown in Eq. (8). To investigate the dependence of k_f on ΔE°, SECM feedback experiments were carried out for ET reactions between tip-generated $ZnPor^+$ in benzene (Eq. (10)) and different aqueous species Red_2 (Eq. (11), where $Red_2 = Ru(CN)_6^{4-}$, $Mo(CN)_8^{4-}$, $Fe(CN)_6^{4-}$, V(II) and Co(II) sepalchrate). The quantitative relation between k_f and the driving force is shown in Fig. 6. Values of k_f were obtained by the best fit of experimental approach curves. The driving force for interfacial ET, $\Delta E^\circ + \Delta^\circ_w\phi$, was obtained from the difference between the $E_{1/2}$ values of Red_2 in water and ZnPor in benzene [17]. Fig. 6 shows that there are two regions for the change of ET rate with driving force. One occurs when the driving force is smaller than ~ 300 mV where $\log k_f$ has a linear relationship with the driving force. The transfer coefficient, α, obtained from the Tafel plots was very close to 0.5. In the other region, above ~ 300 mV, the ET rate was too high to measure and the interfacial reaction rate was governed by diffusion of $ZnPor^+$ in the gap between the tip and the ITIES. The demonstrated dependences of k_f on both ΔE° and $\Delta^\circ_w\phi$ allow us to exclude the possibility that the measured kinetics relate to an IT rather than an ET reaction. For instance, if the transfer of $ZnPor^+$ was rate-limiting, k_f should be independent of ΔE°. If, on the other hand, homogeneous rather than interfacial ET were the slow step, the overall rate would be independent of $\Delta^\circ_w\phi$.

5. Long-range ET through a lipid monolayer at the ITIES

According to Marcus theory [11–13], in the absence of work terms, the energy of activation for an ET reaction is given by:

$$\Delta G^{\neq} = \left(\frac{\lambda}{4}\right)\left(\frac{(1 + \Delta G^\circ)}{\lambda}\right)^2 \quad (12)$$

where λ is the reorganization energy and ΔG° is given by:

$$\Delta G^\circ = -F(\Delta E^\circ + \Delta^\circ_w\phi) \quad (13)$$

According to Eq. (12), the activation energy of the ET reaction depends parabolically on ΔG°, and in the Marcus inverted region at large ΔG° values, increases as the driving force increases. Although Marcus theory has been tested and verified for a number of chemical and biological systems [21], a Marcus inverted region has not been demonstrated at the ITIES. Indeed, in the SECM experiments described above such inverted region behavior could not be seen because with high driving forces, the interfacial ET rate at the ITIES was so fast that the rate was controlled by the diffusion rate (Fig. 6). To observe the inverted region at the ITIES, two methods were used. One was to modify the interface with a phospholipid monolayer as an ET barrier, resulting in slower ET rates that were measurable under

the conditions of the previous SECM experiments [17]. Another was to decrease the concentration of Red_2 in the bottom phase, so that even without a lipid layer at the interface, fast ET rates could be measured [7]; this second approach will be discussed in the next section.

Fig. 7 shows the principles for SECM measurements of ET through an ITIES modified with a lipid monolayer. The ET reactions at the tip and at the ITIES can be expressed by Eqs. (10) and (11) (where $Red_2 = Ru(CN)_6^{4-}$ or $Fe(CN)_6^{4-}$), respectively. After a monolayer was formed at the ITIES, the ET rate was significantly decreased and depended on the lipid concentration and chain length (Fig. 8). The ET rate through the ITIES decreases as the lipid chain length increases. Moreover, for lipid concentrations higher than 50 μM, the ET rate does not change with increasing lipid concentration, suggesting that at these concentrations a complete monolayer has formed at the interface. In ET studies a higher lipid concentration was generally used, so that the rate would not change with small fluctuations in the lipid concentration. Studies were also carried out on the dependence of the ET rate at the ITIES on the structure of the adsorbed phospholipids [22].

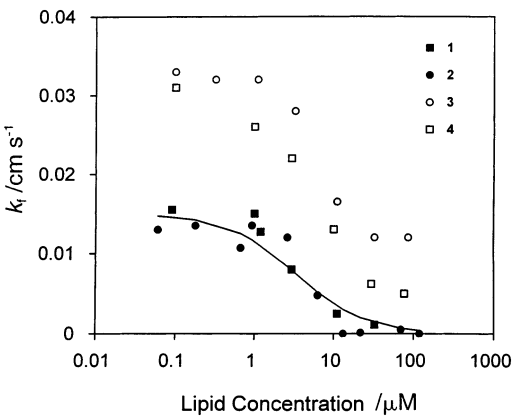

Fig. 8. Dependence of the rate constant of ET between $ZnPor^+$ and $Ru(CN)_6^{4-}$ (■ and ●) or $Fe(CN)_6^{4-}$ (○ and □) on lipid concentration in benzene. The number of methylene groups in the lipid hydrocarbon chain was: 10 (■ and ○), 12 (□), and 20 (●). The organic phase contained 0.25 M $THAClO_4$, 0.5 mM ZnPor, and lipid. The water phase contained 0.1 M NaCl, 0.1 M $NaClO_4$, and 7 mM $Ru(CN)_6^{4-}$ (■ and ●) or $Fe(CN)_6^{4-}$ (○ and □). Rate constants were obtained by fitting experimental approach curves to the theory [5,16]. The solid line represents the Frumkin isotherm with $B = 2 \times 10^5$ M^{-1} and $a = 0.25$ [17]. Reprinted from Ref. [17]. Copyright 1997 American Chemical Society.

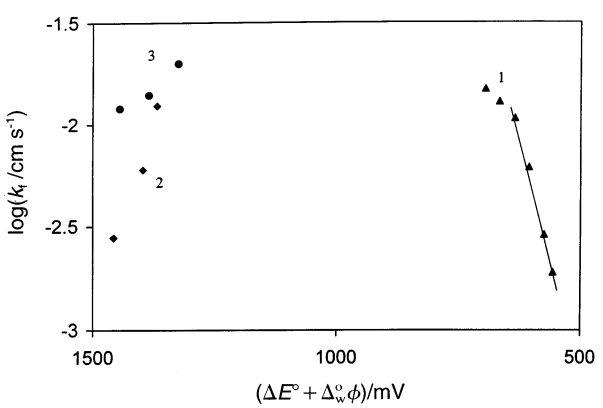

Fig. 9. Driving force dependence of the ET rate between $ZnPor^+$ in benzene and various aqueous redox species across a monolayer of C-10 lipid. The organic phase contained 0.25 M $THAClO_4$, 0.5 mM ZnPor, and 100 M C-10. The aqueous solution contained 7 mM of (1) $Fe(CN)_6^{4-}$, (2) Co(II) sepalchrate, and (3) V^{2+}. Reprinted from Ref. [17]. Copyright 1997 American Chemical Society.

The relation between the driving force and ET rate with different redox couples in the aqueous solution, ZnPor in the non-aqueous phase, and a C-10 lipid monolayer at the water | benzene interface, is shown in Fig. 9. With $Fe(CN)_6^{4-}$, where the difference in half wave potentials between ZnPor and this species is low ($\lesssim 630$ mV), log k_f increased linearly with driving force, giving a slope of $\alpha = 0.59$ for the Tafel plot. With a larger driving force, the ET rate for V(II) and Co(II) sepalchrate decreased with an increase in driving force, as predicted by Marcus theory [21], suggesting inverted region behavior at the ITIES. Note that this result cannot be explained on the basis of the diffuse layer effect [17]. The Marcus inverted region cannot usually be seen at interfaces, such as metal electrodes, because a continuum of electronic states exists in the metal, which allows ET from lower states at high driving potentials. This is not the case at the ITIES, which is closer to the situation for homogeneous ET reactions.

6. SECM measurements of ET reactions at ITIES without the constant composition approximation

As shown in the previous section, the decrease of the ET rate at lipid-modified ITIES allows for accessing ET reactions with large driving forces [17]. On the other hand, SECM measurement of rapid ET kinetics at unmodified ITIES is desirable for a better understanding of these processes. The previous SECM experiments were carried out with a concentration of reactant in phase 2 much higher than that of the mediator in phase 1 (constant composition approximation), so that a simpler theoretical treatment could be used. However, by using lower concentrations of reactant in the second phase, the interfacial ET rate is decreased (Eq. (6)), thus making larger rate constants accessible before diffusion limitations come into play [7]. Unwin and co-workers recently developed a theoretical model that includes depletion and diffusion effects in the second phase for probing the kinetics of partitioning of electroactive solutes between two immiscible phases [23]. The numerical model could be extended straightforwardly for SECM feedback for the case of irreversible

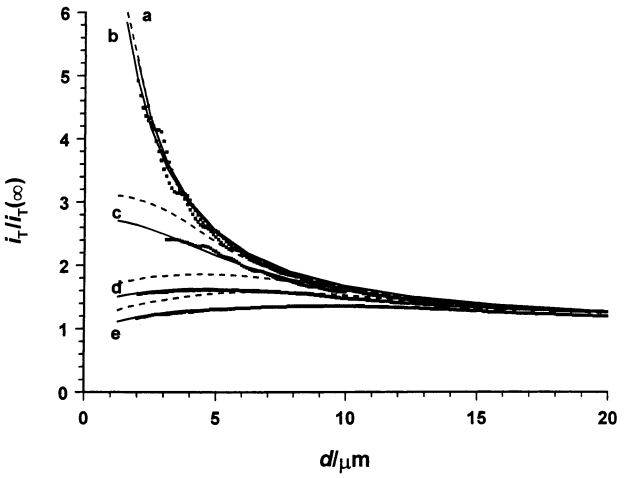

Fig. 10. Experimental approach curves for the oxidation of ZnPor at a tip UME in benzene approaching a benzene | aqueous interface, with the aqueous phase containing $Fe(CN)_6^{4-}$. The bulk concentrations of ZnPor in the organic phase and $Fe(CN)_6^{4-}$ in the aqueous phase were, respectively: (a) 0.500 and 7.00; (b) 0.500 and 3.50; (c) 0.380 and 0.700; (d) 0.380 and 0.350, and (e) 0.380 and 0.255 mM. The solid lines show the behavior predicted for $D_{ZnPor}/D_{Fe(CN)6^{4-}} = 1.7$ and a bimolecular rate constant, $k_{12} = 91$ cm s^{-1} M^{-1}, while the dashed lines show the behavior for a diffusion-controlled process for each of the five cases considered, simulated using the model described in Ref. [7]. The diffusion-controlled characteristics for the two cases with the highest K_r ($= c_{Fe(CN)_6^{4-}}/c_{ZnPor}$) are indistinguishable. Reprinted from Ref. [7]. Copyright 1999 American Chemical Society.

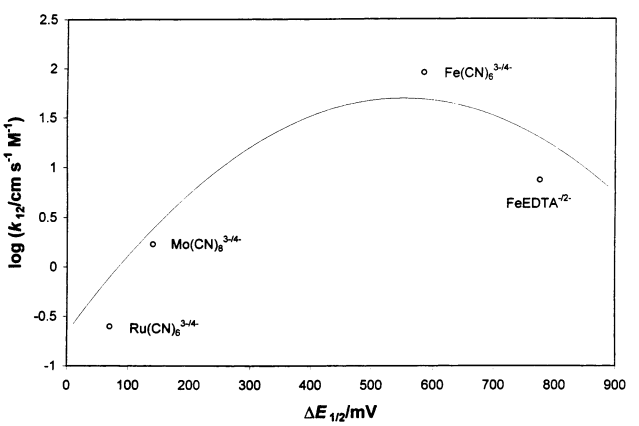

Fig. 11. Plot of $\log k_{12}$ vs. $\Delta E_{1/2}$ derived from the data for the four aqueous reactants. The solid line is expected behavior based on Marcus theory for $\lambda = 0.55$ eV and a maximum rate constant of 50 cm s^{-1} M^{-1}. Reprinted from Ref. [7]. Copyright 1999 American Chemical Society.

ET processes at ITIES (Fig. 2). The more general theory also enables one to identify when the constant composition approximation is valid. Furthermore, the use of relatively low concentrations of the reactant in the second phase was theoretically predicted to have considerable advantages for lowering the ET reaction rate and causing the approach curves in the fast kinetic limit to be more readily distinguished from one another. Indeed, the two advantages were experimentally confirmed as shown below.

Fig. 10 shows a set of approach curves for the reaction between $ZnPor^+$ and $Fe(CN)_6^{4-}$ at the benzene | water interface (Eq. (11)). For the two higher concentration ratios (curves a and b), the interfacial redox reaction appears to be diffusion-controlled and the rate constant cannot be determined, as shown for the same system in previous SECM investigations (Fig. 6) [17]. However, for the lower three concentration ratios (curves c–e), the experimental approach curves lie below the simulated characteristics for a diffusion-controlled process. An analysis of the three approach curves gives a unique rate constant, $k_{12} = 91$ cm s^{-1} M^{-1}. Furthermore, as theoretically predicted, the two approach curves with the lower concentration ratios (curves d and e) flatten and peak as the tip–interface separation is decreased. This effect allows one to distinguish the two approach curves from one another, even when the two curves with the higher concentration ratios (curves a and b) are different only at small d. In the former two curves, the magnitude of the peak current alone is an unequivocal measure of the ET kinetics. Therefore, uncertainties in d, which are frequently encountered in the SECM experiments, become less important.

Analogous experiments were performed for the ET reaction between $ZnPor^+$ in benzonitrile and different redox species, i.e. $Ru(CN)_6^{4-}$, $Mo(CN)_8^{4-}$, and $FeEDTA^{2-}$, in the aqueous phase (Eq. (11)). For each of the systems, a unique rate constant was obtained from approach curves with different concentrations of the aqueous redox species. The results are summarized in a plot of $\log k_{12}$ versus driving force (Fig. 11). For the three systems measured in benzonitrile, $\log k_{12}$ appears to be significantly dependent on the driving force, $\Delta E_{1/2} = \Delta E° + \Delta^o_w\phi$ [17]. Although the solvent used for the $Fe(CN)_6^{4-}$ study was different from that of the other three reactants, the overall trend is consistent with the prediction of Marcus theory [21], showing first an increase in the reaction rate with increasing driving force, followed by a decrease in the inverted region. Observation of the inverted region behavior suggested by these studies is consistent with a recent observation of electrogenerated chemiluminescence at unmodified ITIES [24]. Further SECM studies of ET with larger driving forces are underway using the methodology and theory outlined in this section to obtain more data points with a single solvent system (unpublished results).

7. ET reaction at the micro-ITIES and its use as a probe in SECM for imaging purposes

Based on the ET reaction at ITIES, as in Eq. (2), a micro-interface formed at the tip of a glass capillary of submicrometer dimensions can be used as the imaging

probe of a microband array on a substrate [25]. The glass capillary was filled with an aqueous solution of a redox couple and a supporting electrolyte. The substrate was immersed in an organic solution that is immiscible with water and contained the species of the second redox couple. When a Galvani potential difference was applied, the current was controlled by the rate of ET at the water | organic interface, which in turn is a function of the feedback between the tip and substrate. The micropipet was first lowered to the surface to be imaged until a positive or negative feedback was detected, corresponding to a conducting or insulating part of the substrate structure. SECM images using such micro-ITIES with different capillary diameters were obtained for substrates such as silicon with parallel platinum bands and a corroded strip of copper on a plastic base [25]. Thus, a micro-ITIES can be employed instead of a metallic ultramicroelectrode for imaging purposes in SECM. It is also much easier to fabricate a glass capillary with a small tip diameter than a metallic microelectrode tip.

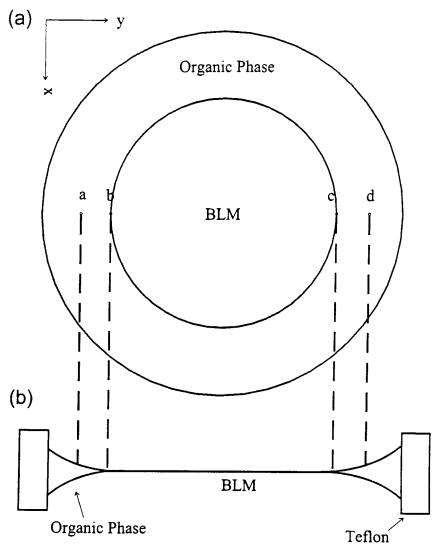

Fig. 12. Top (a) and side (b) views of schematic diagram for the measurement of the approach curves and topographical images of the BLM by SECM. For the latter, the tip approached to close proximity of the surface at point a and was then scanned toward point d (a → b → c → d) at a constant height. Teflon membrane thickness, 150 μm. Reprinted from Ref. [30]. Copyright 1999 American Chemical Society.

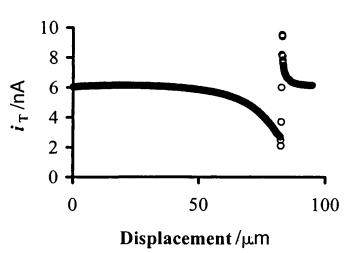

Fig. 13. Current approach curve obtained at the 25 μm diameter Pt SECM tip as the tip–BLM separation was reduced. The BLM was formed from a solution of lecithin (1.25 mg ml^{-1}) in *n*-heptane. The aqueous solution contained 1 mM $Ru(NH_3)_6^{3+}$ as the electroactive species, with 0.1 M KCl as supporting electrolyte. The tip potential was −0.35 V vs. the Ag | AgCl reference electrode. Reprinted from Ref. [30]. Copyright 1999 American Chemical Society.

8. Application of SECM to the study of charge transfer through bilayer lipid membranes

8.1. SECM studies of insulating BLMs

Although the ITIES has been proposed as a model system for a biological membrane, it really differs in many respects from an actual membrane, even when a lipid monolayer is present at the interface. For example, a key feature of biological membranes is the presence of selective channels that permit transport of ions and neutral molecules across the membrane. These are not easily studied at the ITIES. A better alternative model is the planar BLM [26,27]. Because of the self-assembled bilayer structures, the BLM is more suitable for the study of the electrical properties of membrane-bound components that control ion- and electron-transfer across biological membranes. Furthermore, the apparently opposite properties of ion-transfer across BLMs and the ITIES have been pointed out recently [28]. We have recently started experiments on the use of SECM to study charge transfer processes across BLMs [29]. For previous work using potentiometric and amperometric microelectrodes to extract kinetic information of ion transport across BLMs see Refs. [30–33].

The permeability of hydrophilic ions through unmodified BLMs is known to be very low. This insulating property of an unmodified BLM was investigated with the SECM. The Pt UME tip was moved toward the BLM (*z*-direction) and scanned horizontally (*x*- or *y*-direction) in close proximity to the BLM (Fig. 12). As opposed to a conventional BLM apparatus, where the membrane is oriented vertically, the BLM was horizontally oriented to make the cell compatible with the usual SECM apparatus. This design requires provision that pressure gradients, which would lead to rupture of the BLM, do not form. Fig. 13 shows a typical experimental approach curve with $Ru(NH_3)_6^{3+}$ as a mediator. As the BLM is approached in the *z*-direction, the tip current decreases from its diffusion-limited value, $i_{T,\infty}$, toward zero. The declining portion of the approach curve fits well with the theoretical curve assuming purely negative feedback [34], indicating that the BLM was completely insulating under these conditions. When the tip contacted the membrane the tip current increased and then transiently decayed back to the $i_{T,\infty}$ value, as expected for the tip contacting fresh solution of the same composition as in the upper compartment. This indicates that the membrane is broken

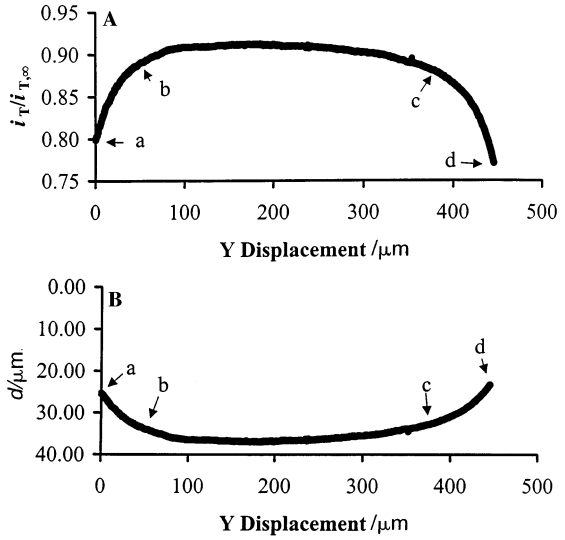

Fig. 14. Transport-limited current image (A) and the corresponding topographical image (B) of a bilayer obtained by scanning 25 μm diameter Pt SECM tip along one axis parallel to the surface in a solution containing 1 mM $Fe(CN)_6^{4-}$ and 0.1 M NaCl. Tip potential, 0.4 V vs. Ag | AgCl, scan rate 3 μm s^{-1}. The indicated points, a–d, correspond to the positions in Fig. 12, as observed by optical microscopy. Reprinted from Ref. [30]. Copyright 1999 American Chemical Society.

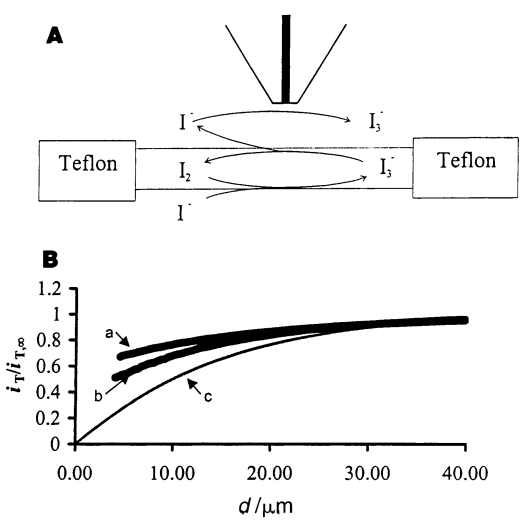

Fig. 15. (A) Processes at BLMs for I^-/I_2 mediator oxidized at the tip. (B) Analysis of approach curves for the oxidation of 2.53 mM I^- in 0.1 M KCl with bilayer prepared with lipid from (a) 18 and (b) 9 mM solutions of I_2 in *n*-heptane. The solid line (c) represents SECM theory for an insulating substrate [34]. Reprinted from Ref. [30]. Copyright 1999 American Chemical Society.

by the contact and that the tip contacted with the lower solution and reformed a steady-state concentration profile.

The BLM was formed by spreading a thin film of a lipid across a small (~ 600 μm diameter) hole in a 150 μm thick Teflon membrane. The shape of the structure that forms in the hole consists of a BLM (two molecular layers thick) in the middle of the membrane, surrounded by a thicker torus-shaped layer in contact with the Teflon support. To obtain the topographic image of the BLM surrounded by the annulus (Fig. 12), the SECM tip was scanned horizontally across the BLM including the annulus region. $Fe(CN)_6^{4-}$, employed as a mediator, showed negative feedback at both the BLM and the annulus. The UME tip was moved in the *z*-direction into close proximity of the annulus surface (point a in Fig. 12) until the current flowing at the electrode decreased to about 0.80 $i_{T,\infty}$. Then, the tip was scanned toward the opposite side of the annulus over the bilayer (a → b → c → d in Fig. 12) at a constant height. The position of the tip was simultaneously observed with an optical microscope. As shown in Fig. 14(A), at all tip positions, the current detected was smaller than $i_{T,\infty}$, indicating that the tip was always in close proximity to the surface. The diffusion-limited current image (Fig. 14(A)) was converted into a topographical image (Fig. 14(B)) on the basis of the theoretical equation for negative feedback. Fig. 14(B) shows the SECM topographical image of a bilayer surrounded by the annulus. The diameter of the bilayer region that was estimated from Fig. 14(B) (~ 350 μm) agrees well with that observed by optical microscopy.

8.2. Ion transfer across BLMs

Although unmodified BLMs behave as insulators for hydrophilic ions, BLMs modified with certain lipophilic molecules that can form channels or act as carriers show high permeability toward hydrophilic ions. Similarly, certain lipophilic molecules in the BLM can mediate ET between reactants that are located on the opposite sides of the membrane. For example, the BLM permeability toward I^- has previously been shown to increase in the presence of I_2 [35]. The main pathway is likely to be a facilitated transfer of I^- by I_2 forming I_3^- in the membrane (Fig. 15(A)), although an electron transfer at both interfaces by membrane I_2 is also an alternative pathway. Therefore, I^- was used as a redox mediator for SECM studies of BLMs modified with I_2. Fig. 15(B) clearly shows that, as the BLM modified with I_2 was approached, the tip current was higher than that expected for negative feedback and found with mediators like $Fe(CN)_6^{4-}$. These results imply that the depletion of I^- by oxidation at the SECM tip induced a transfer of I^- across the BLM. A higher concentration of I_2 in the BLMs results in large positive feedback, indicating faster transfer of I^- across the BLM. To understand the SECM-induced I^- transfer across the BLM quantitatively, the rate constant was determined on the basis of the model that was recently developed by Unwin and co-workers [23]. For simplicity, I^- transfer between the two aqueous phases was assumed to be characterized by the first-order rate

constant, k. Comparison of the calculated approach curves in Ref. [23] with, for example, the experimental data for the BLM with 18 mM I_2 gives a value of about 0.01 cm s^{-1} for k. In contrast to a previous report on this system [36], the fast kinetic parameter could be extracted by SECM. Ion transfer across BLMs can also be mediated by molecules that form channels in the membranes. A number of isolated channel proteins and their peptide analogues have been reconstituted into planar BLMs and the structure–function relationships of such ion channels have been studied [37]. Importantly, many of the ion-channels and their peptide analogues selectively mediate the transfer of small ions that are electrochemically inactive, e.g. Na^+, K^+, Ca^{2+}, and Cl^-. Therefore, ion-selective micropipet electrodes, rather than conventional metal microelectrodes, were used as an SECM tip to study channel-mediated ion transfer across BLMs. The pipes were filled with an organic solution of a ligand molecule, i.e. an ionophore [38], that selectively forms complexes with the analyte of interest. Thus, the ionophore-facilitated transfer of an ion from the outer aqueous solution into the pipet results in a well-defined tip current [39,40]. As a K^+-selective micropipet electrode based on valinomycin approached the BLMs incorporating gramicidin as an ion-channel forming peptide [41], the K^+-flux through the peptide pores was detected as a positive feedback current. Details of these studies will be presented elsewhere (unpublished results).

9. Conclusions

SECM is a powerful technique to understand quantitatively the dynamics of heterogeneous ET reactions at the ITIES. The SECM feedback experiments of ET reactions at ITIES: (i) allow discrimination between ET and IT processes at the interface; (ii) eliminate distortions associated with *IR* drop and charging current, and (iii) avoid complications due to the limited potential window of the ITIES. Furthermore, in SECM experiments the diffusion of the reactants from the bulk water and organic phases to the interface is well-defined and calculable. Thus, ET rate constants at ITIES, which previously have been difficult [42], can be accurately determined with the SECM. Application of the SECM to the ET studies at ITIES has also resulted in development of analogous techniques, like measurements in drops of immiscible liquids [43] or thin immiscible liquid films on surfaces [44] that also provide information about ET dynamics at the ITIES. The ET reaction mechanisms at ITIES, which have been treated theoretically [42], can now be discussed on the basis of the experimental data that are obtained with the SECM and analogous techniques, as well as with recently developed spectroelectrochemical and photoelectrochemical techniques [45,46], where photoexcitation of one of the reactants can increase the driving force of the ET without the limitation of the potential window.

The SECM feedback experiments and the theory developed for ITIES studies are also applicable to determine charge-transfer kinetics across BLMs. In addition to kinetic measurements, SECM observation of a single ion-channel in a BLM is an exciting goal of our studies [47]. The SECM may allow for electrochemical detection and location of a single ion-channel in a BLM, since these should show a reasonably high conductivity (as shown by patch clump experiments [48]) and relatively slow lateral-diffusion in the membrane ($D = 10^{-7}$–10^{-9} cm^{-2} s^{-1} [49]).

Acknowledgements

The contributions of Michael V. Mirkin, Theodros Solomon, Michael Tsionsky, Chang Wei, Marie-Hélène Delville, Patrick R. Unwin, Anna L. Barker, Robert A.W. Dryfe, and Fu-Ren F. Fan and the support of this research by grants from the Robert A. Welch Foundation and the National Science Foundation are gratefully acknowledged. S.A. expresses thanks for a postdoctoral fellowship from the Japan Society for the Promotion of Science.

References

[1] H.H. Girault, D.J. Schiffrin, in: A.J. Bard (Ed.), Electroanalytical Chemistry, vol. 15, Marcel Dekker, New York, 1989, p. 1.
[2] A.J. Bard, F.-R.F. Fan, M.V. Mirkin, in: A.J. Bard (Ed.), Electroanalytical Chemistry, vol. 18, Marcel Dekker, New York, 1993, p. 243.
[3] A.J. Bard, F.-R.F. Fan, M.V. Mirkin, in: I. Rubinstein (Ed.), Physical Electrochemistry: Principles, Methods and Applications, Marcel Dekker, New York, 1995, p. 209.
[4] T. Kakiuchi, in: A.G. Volkov, D.W. Deamer (Eds.), Liquid–Liquid Interfaces: Theory and Methods, CRC Press, New York, 1996, p. 1.
[5] C. Wei, A.J. Bard, M.V. Mirkin, J. Phys. Chem. 99 (1995) 16033.
[6] C.P. Andrieux, J. Savéant, in: R.W. Murray (Ed.), Molecular Design of Surfaces, Wiley, New York, 1992, p. 207.
[7] A.L. Barker, P.R. Unwin, S. Amemiya, J.F. Zhou, A.J. Bard, J. Phys. Chem. B 103 (1999) 7260.
[8] V.J. Cunnane, D.J. Schiffrin, C. Beltran, G. Geblewicz, T. Solomon, J. Electroanal. Chem. 247 (1988) 203.
[9] K. Maeda, S. Kihara, M. Suzuki, M. Matsui, J. Electroanal. Chem. 303 (1991) 171.
[10] T. Kakiuchi, Electrochim. Acta 40 (1995) 2999.
[11] R.A. Marcus, J. Phys. Chem. 94 (1990) 1050.
[12] R.A. Marcus, J. Phys. Chem. 94 (1990) 4152.
[13] R.A. Marcus, J. Phys. Chem. 95 (1991) 2010.
[14] H.H. Girault, D.J. Schiffrin, J. Electroanal. Chem. 244 (1988) 15.
[15] H.H. Girault, J. Electroanal. Chem. 388 (1995) 93.
[16] M. Tsionsky, A.J. Bard, M.V. Mirkin, J. Phys. Chem. 100 (1996) 17881.

[17] M. Tsionsky, A.J. Bard, M.V. Mirkin, J. Am. Chem. Soc. 119 (1997) 10785.
[18] T. Solomon, A.J. Bard, J. Phys. Chem. 99 (1995) 17487.
[19] B. Liu, M.V. Mirkin, J. Am. Chem. Soc. 121 (1999) 8352.
[20] A.J. Bard, L.R. Faulkner, Electrochemical Methods, Wiley, New York, 1980, p. 540.
[21] R.A. Marcus, N. Sutin, Biochim. Biophys. Acta 811 (1985) 265.
[22] M. Delville, M. Tsionsky, A.J. Bard, Langmuir 14 (1998) 2774.
[23] A.L. Barker, J.V. Macpherson, C.J. Slevin, P.R. Unwin, J. Phys. Chem. B 102 (1998) 1586.
[24] Y. Zu, F.-R.F. Fan, A.J. Bard, J. Phys. Chem. B 103 (1999) 6272.
[25] T. Solomon, A.J. Bard, Anal. Chem. 67 (1995) 2787.
[26] R.B. Gennis, Biomembranes: Molecular Structure and Function, Springer-Verlag, New York, 1989.
[27] W. Hanke, W. Schlue, Planar Lipid Bilayers: Methods and Applications, Academic Press, London, 1993.
[28] T. Kakiuchi, Electrochim. Acta 44 (1998) 171.
[29] M. Tsionsky, J.F. Zhou, S. Amemiya, F.-R.F. Fan, A.J. Bard, R.A.W. Dryfe, Anal. Chem. 71 (1999) 4300.
[30] Y.N. Antonenko, A.A. Bulychev, Biochim. Biophys. Acta 1070 (1991) 279.
[31] P. Pohl, S.M. Saparov, Y.N. Antonenko, Biophys. J. 75 (1998) 1403.
[32] H. Yamada, T. Matsue, I. Uchida, Biochem. Biophys. Res. Commun. 180 (1991) 1330.
[33] T. Matsue, H. Shiku, H. Yamada, I. Uchida, J. Phys. Chem. 98 (1994) 11001.
[34] M.V. Mirkin, F.-R.F. Fan, A.J. Bard, J. Electroanal. Chem. 328 (1992) 47.
[35] C.J. Bender, H.T. Tien, Anal. Chim. Acta 201 (1987) 51.
[36] P. Läuger, J. Richter, W. Lesslauer, Ber. Bunsen-Ges. Phys. Chem. 71 (1967) 906.
[37] C. Miller, Ion Channel Reconstitution, Plenum, New York, 1986.
[38] P. Bühlmann, E. Pretsch, E. Bakker, Chem. Rev. 98 (1998) 1593.
[39] Y. Shao, M.V. Mirkin, Anal. Chem. 70 (1998) 3155.
[40] Y. Shao, M.V. Mirkin, J. Phys. Chem. B 102 (1998) 9915.
[41] G.A. Woolley, B.A. Wallace, J. Membr. Biol. 129 (1992) 109.
[42] H.H. Girault, in: R.E. White, B.E. Conway, J.O'M. Bockris (Eds.), Modern Aspects of Electrochemistry, vol. 25, Plenum, New York, 1993, p. 1.
[43] J. Zhang, C.J. Slevin, P.R. Unwin, Chem. Commun. (1999) 1501.
[44] C. Shi, F.C. Anson, J. Phys. Chem. B 103 (1999) 6283.
[45] Z. Ding, D.J. Fermín, P. Brevet, H.H. Girault, J. Electroanal. Chem. 458 (1998) 139.
[46] D.J. Fermín, H.D. Duong, Z. Ding, P. Brevet, H.H. Girault, Phys. Chem. Chem. Phys. 1 (1999) 1461.
[47] A.J. Bard, F.-R.F. Fan, Acc. Chem. Res. 29 (1996) 572.
[48] B. Sakmann, E. Neher, Single-Channel Recording, 2nd ed., Plenum, New York, 1995.
[49] D.A. Jans, The Mobile Receptor Hypothesis: The Role of Membrane Receptor Lateral Movement in Signal Transduction, Chapman and Hall, New York, 1997.